

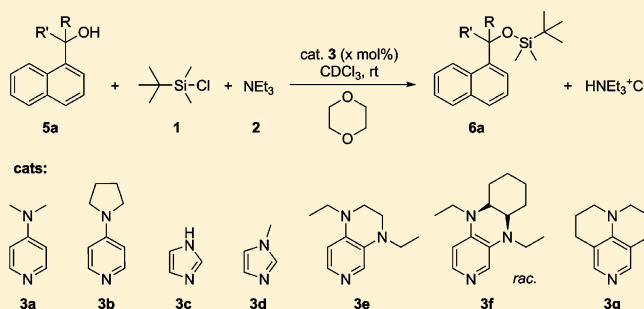
The Lewis Base-Catalyzed Silylation of Alcohols—A Mechanistic Analysis

Pascal Patschinski, Cong Zhang, and Hendrik Zipse*

Department of Chemistry, Ludwig-Maximilians-Universität, 81377 München, Germany

S Supporting Information

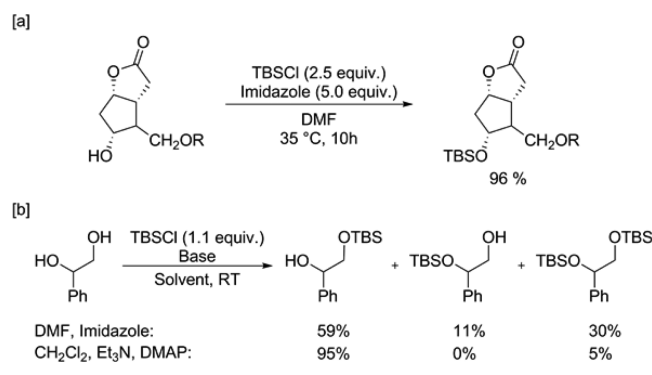
ABSTRACT: Reaction rates for the base-catalyzed silylation of primary, secondary, and tertiary alcohols depend strongly on the choice of solvent and catalyst. The reactions are significantly faster in Lewis basic solvents such as dimethylformamide (DMF) compared with those in chloroform or dichloromethane (DCM). In DMF as the solvent, the reaction half-lives for the conversion of structurally similar primary, secondary, and tertiary alcohols vary in the ratio 404345:20232:1. The effects of added Lewis base catalysts such as 4-*N,N*-dimethylaminopyridine (DMAP) or 4-pyrrolidinopyridine (PPY) are much larger in apolar solvents than in DMF. The presence of an auxiliary base such as triethylamine is required in order to drive the reaction to full conversion.



INTRODUCTION

The silylation of hydroxyl groups represents one of the most important protecting-group strategies in the manipulation of polyfunctional molecules.^{1–3} The usefulness of this reaction was demonstrated by Venkateswarlu and Corey in 1972 using *tert*-butyldimethylsilyl chloride (TBSCl, **1**) in DMF as the solvent with imidazole as the base and catalyst for the protection of secondary alcohols (Scheme 1a).⁴ In the same

Scheme 1. (a) Protection of a Secondary Alcohol Using Corey's Method;⁴ (b) Selectivity in the Silylation of Unsymmetric 1,2-Diols⁵



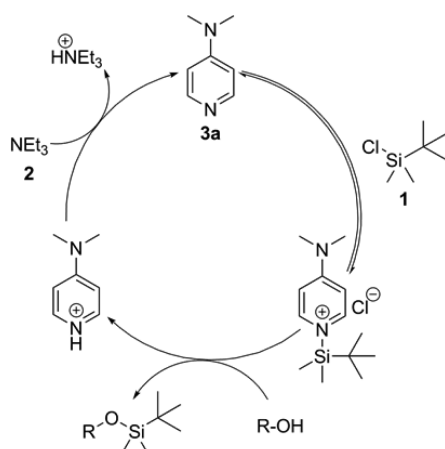
report it was also demonstrated that TBS ethers can be cleaved effectively under mild conditions using tetra-*N*-butylammonium fluoride in THF. This “Corey method” has since been applied to a multitude of substrates containing (mainly) primary and secondary hydroxyl groups, thus documenting its general usefulness.

A number of alternative protocols have also been explored using different combinations of bases and/or solvents, such as those by Hernandez [triethylamine (Et₃N, **2**)/4-*N,N*-dimethylaminopyridine (DMAP, **3a**)],⁵ Chang (Et₃N/1,1,3,3-tetramethylguanidine and Et₃N/DBU),⁶ Weiffen (18-crown-6/K₂CO₃),⁷ Lombardo [*i*-Pr₂NEt (**4**)],⁸ and Fuchs (18-crown-6/KH).⁹ The first two of these studies employ catalyst systems closely related to that used in the Corey procedure, as both employ a nitrogen heterocycle as the actual catalytic base. Despite this apparent similarity, the reaction catalyzed by DMAP in apolar organic solvents shows higher selectivities in the transformation of polyol substrates carrying primary and secondary hydroxyl groups (Scheme 1b). As shown in Scheme 2 for the example of DMAP, catalytic Lewis bases are believed to react with silyl chlorides to form silylpyridinium ion pairs, whose subsequent reaction with the alcohol substrate yields the silyl ether products together with the protonated (and thus deactivated) pyridine base.¹⁰ Reactivation of the catalyst then requires the action of an auxiliary base such as **2**.

This mechanism is practically identical to the consensus mechanism for the pyridine-catalyzed acylation of alcohols employing anhydrides as acylating reagents.^{11–13} For these acylation reactions, more electron-rich (and thus more active) pyridines have recently^{14–16} been developed through extension of the DMAP structure, and here we explore the usefulness of these catalysts for the silylation of primary, secondary, and tertiary alcohols.

Received: July 22, 2014

Published: July 31, 2014

Scheme 2. Mechanism of the DMAP-Catalyzed Silylation of Alcohols⁵

RESULTS AND DISCUSSION

Reaction with Primary Alcohol 5a. Initial experiments were performed for the reaction of naphthalen-1-ylmethanol (5a) with 1 (1.2 equiv) and 2 (1.2 equiv) as the auxiliary base in CDCl₃ using different nucleophilic catalysts, as depicted in Figure 1. Dioxane was added as an internal standard. The progress of the silylation reaction was monitored by ¹H NMR spectroscopy, and initial attempts were devoted to calibration of the signals of alcohol 5a and its silyl ether 6a. The signal of the CH₂ group of the alcohol, however, was found to shift in an unfavorable manner as the reaction progressed, making it unsuitable for full kinetic analysis. The methyl group signals of the silyl group were found to be more useful in this respect, and a practical protocol was developed to monitor the reaction progress to near completion (see the Supporting Information for details). On closer inspection, all of the ¹H NMR spectra obtained under the reaction conditions indicated the presence of small amounts of bis(silyl) ether 7 (Figure 2). In experiments with defined amounts of added water, 7 was rapidly generated from 2 equiv of silyl chloride 1 and 1 equiv of water. These results show that the reactions in the following mechanistic studies contain no more than 2% water. The conversion of silyl chloride 1 follows an effective rate law involving first-order behavior of all of the reactants and the catalyst and zeroth-order behavior of the auxiliary base (see the Supporting Information for full information). The conversion

of silyl chloride 1 (Figure 3) and the appearance of silylated alcohol 6a could be fitted using an effective second-order rate law. The corresponding effective rate constant k_{eff} could then be used to characterize the reaction in terms of its effective reaction half-life $t_{1/2}$ (see the Supporting Information for details).

It was recently shown for acylation reactions that the auxiliary base plays an important role in maintaining the catalyst activity over many turnover cycles.¹¹ This point was therefore tested in the silylation reaction (Figure 1) with 4 mol % DMAP in the presence of different amounts of auxiliary base. As can readily be seen from the turnover curves in Figure 4, the rates of silylation were practically identical for the reactions involving 2.2, 1.7, and 1.2 equiv (relative to alcohol 5a) of Et₃N as the auxiliary base. This implies that the auxiliary base is not directly involved in the catalytic cycle but merely needed to regenerate the catalyst. When too little auxiliary base is present for this latter task, the reaction slows down dramatically after a certain percentage of turnover (as is visible from the turnover curve for 0.7 equiv of Et₃N). In the absence of auxiliary base, the reaction is extremely slow and not easily analyzed in terms of a second-order rate law. Thus, we conclude that silylation reactions such as the one described in Figure 1 are best run in the presence of 1.2 equiv of the auxiliary base.

The effectiveness of Et₃N (2) as an auxiliary base for the silylation was subsequently explored by rerunning the benchmark reaction using other auxiliary bases such as trioctylamine (TOA, 8), *N,N*-diisopropylethylamine (DIPEA, 4), 1,4-diazabicyclo[2.2.2]octane (DABCO, 9), 1,8-bis-(dimethylamino)naphthalene (Proton Sponge, 10), and *N*-methylmorpholine (NMM, 11). The results compiled in Table 1 show nearly no variation in the reaction half-life among bases with similar pK_a values, such as DIPEA (30.7 min), TOA (30.5 min), and Et₃N (30.2 min).

The true advantage of TOA over the other two bases clearly lies in the much better solubility of its ammonium chloride salt in organic solvents. The reaction with NMM, an amine of lower basicity, led to a significantly extended reaction half-life (127.7 min). Under these conditions, regeneration of DMAP (with $pK_a = 9.7$) is not effective anymore.¹⁸ Despite its low basicity, DABCO (9) is quite efficient in its ability to promote the silylation reaction, with $t_{1/2} = 26.5$ min. However, this latter result more likely reflects its activity as a catalytic Lewis base rather than its ability to regenerate protonated DMAP (in line with earlier studies of the kinetic and thermodynamic basicities

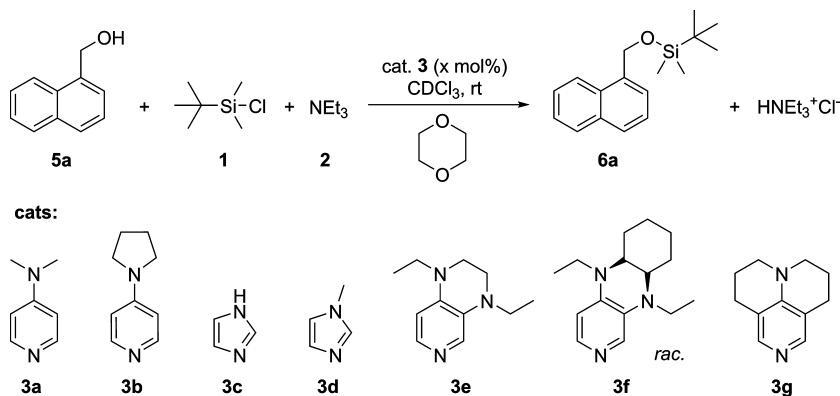


Figure 1. Silylation of naphthalen-1-ylmethanol (5a) with TBSCl (1) and Et₃N (2) in CDCl₃ together with structures of all of the catalysts used (3a–g).

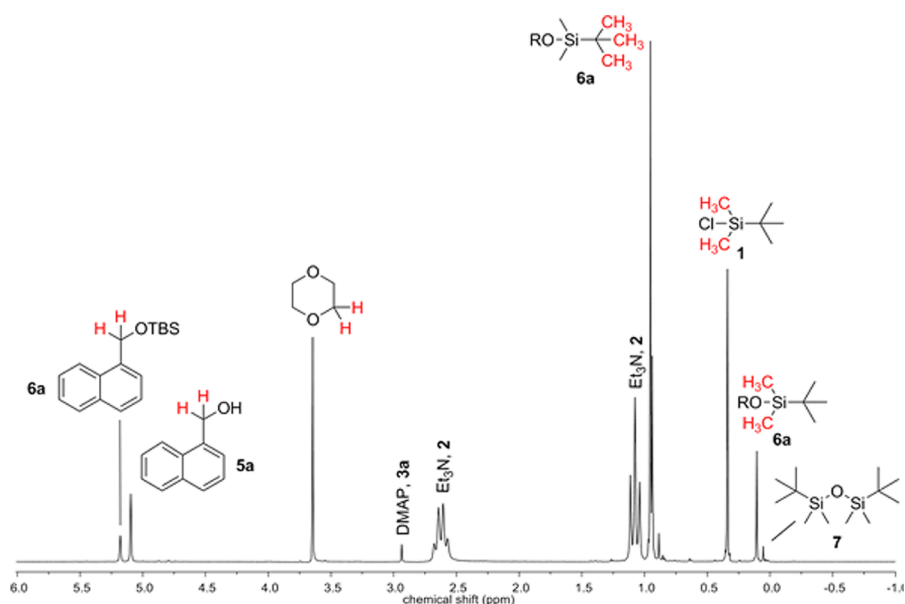


Figure 2. ^1H NMR spectra of the benchmark reaction in CDCl_3 using the primary alcohol **5a**, **2** as the auxiliary base, and DMAP as the catalyst.

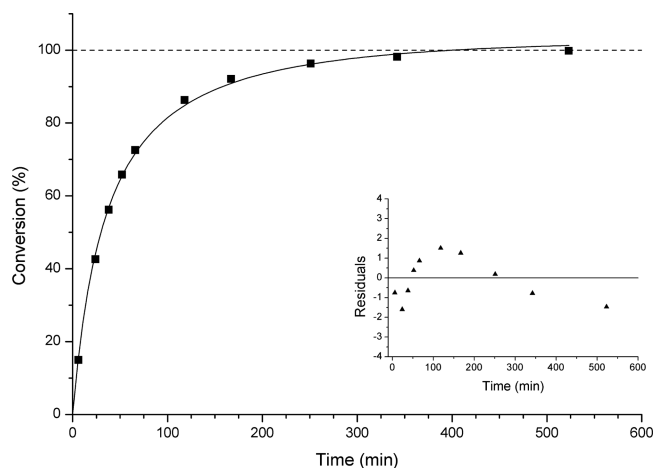


Figure 3. Silylation of alcohol **5a** with **1** (1.2 equiv) using **2** (1.2 equiv) as the base and DMAP (4 mol %) as the catalyst in CDCl_3 as monitored by ^1H NMR spectroscopy.

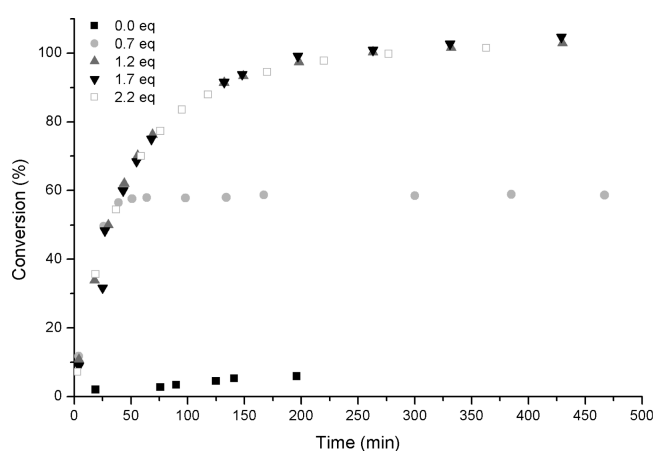


Figure 4. Turnover curves for the silylation of alcohol **5a** catalyzed by 4 mol % DMAP in the presence of variable concentrations of Et_3N (**2**) in CDCl_3 as monitored by ^1H NMR spectroscopy.

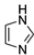
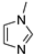
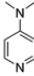
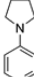
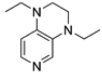
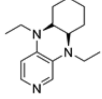
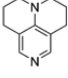
Table 1. Rate Data for the Silylation of Alcohol **5a** Using DMAP (4 mol %) as the Catalyst with Various Auxiliary Bases (1.2 equiv) in CDCl_3

auxiliary base	$\text{p}K_{\text{a}}(\text{H}_2\text{O})^{25}$	$k_{\text{eff}}^{[\text{a}]}$	$t_{1/2}^{[\text{b}]}$	
no base		$4.10 \cdot 10^{-3}$	187.3 ^[c]	
	11	7.80 ^[19]	$6.01 \cdot 10^{-3}$	127.7
	9	8.70 ^[20]	$2.90 \cdot 10^{-2}$	26.5
	8	11.19 ^[21]	$2.52 \cdot 10^{-2}$	30.5
	4	11.44 ^[22]	$2.50 \cdot 10^{-2}$	30.7
	2	11.58 ^[23]	$2.54 \cdot 10^{-2}$	30.2
	10	12.10 ^[24]	$2.05 \cdot 10^{-2}$	37.4

^a k_{eff} in $\text{L} \cdot \text{mol}^{-1} \cdot \text{s}^{-1}$. ^bHalf-life in min. ^cOnly 7% conversion.

of DABCO).¹⁷ Why the reaction slows down somewhat with Proton Sponge (**10**) as the auxiliary base ($t_{1/2} = 37.4$ min) is not immediately evident from the aqueous-phase $\text{p}K_{\text{a}}$ values. Reaction half-lives were determined for all of the catalysts shown in Figure 1, including DMAP, PPY (**3b**), imidazole (**3c**), and *N*-methylimidazole (**3d**) as well as the electron-rich pyridines **3e**, **3f**, and **3g** recently developed for acylation reactions (Table 2).^{14,25} All of the benchmark experiments were performed at a catalyst loading of 4 mol %. The least efficient catalyst ($t_{1/2} = 163.9$ min) is imidazole (**3c**), which is used in large excess in the original Corey procedure. This is approximately 5 times slower than the reaction with DMAP

Table 2. Silyl Cation Affinities (SCAs) and Rate Data for the Silylation of Alcohol **5a** Using Different Lewis Base Catalysts at 4 mol % Catalyst Loading

Catalyst	SCA ^[a] [Gas]	SCA ^[b] [Solv]	$k_{\text{eff}}^{\text{[c]}}$	$t_{1/2}^{\text{[d]}}$
 3c	-20.0	-24.7	$4.69 \cdot 10^{-3}$	163.9 ± 2.3
 3d	-36.4	-32.4	$1.17 \cdot 10^{-2}$	65.9 ± 3.3
 3a	-57.0	-43.1	$2.54 \cdot 10^{-2}$	30.2 ± 1.4
 3b	-64.8	-47.4	$3.90 \cdot 10^{-2}$	19.7 ± 0.4
 3e	-83.4	-58.5	$5.30 \cdot 10^{-2}$	14.5 ± 0.3
 3f	-93.2	-62.0	$8.18 \cdot 10^{-2}$	9.4 ± 0.6
 3g	-75.6	-56.5	$8.49 \cdot 10^{-2}$	9.0 ± 0.5

^aSilyl cation affinities at 298.15 K (in kJ/mol) were calculated at the MP2(FC)/G3MP2large//MPW1K/6-31+G(d) level of theory. ^bSolvation energies were calculated at the PCM/UAHF/MPW1K/6-31+G(d) level of theory for CHCl₃. ^c k_{eff} in L·mol⁻¹·s⁻¹. ^dHalf-life in min.

(30.2 min) and about 18 times slower than the reaction with the most efficient catalyst, **3g** ($t_{1/2} = 9.0$ min).

For the reactions catalyzed by DMAP, PPY, **3d**, **3f**, and **3g**, rate measurements were repeated at different catalyst concentrations, and a clear linear correlation between the rate constant k_{eff} and the catalyst loading was observed in all cases (Figure 5). As was previously found for other Lewis base-catalyzed reactions such as the aza-Morita–Baylis–Hillman reaction and in acylation reactions,^{13,26} this implies that only one catalyst molecule participates in the rate-limiting step. The slope of the correlation line (k'_{eff} ; see Table 3) reflects the intrinsic catalytic efficiency of the catalyst, while the intercept (b) represents the rate of the background reaction in the absence of catalyst (eq 1).

$$k_{\text{eff}} = k'_{\text{eff}}[\text{cat}] + b \quad (1)$$

Visual inspection of Figure 5 indicates that the rate of the background reaction is quite small. This point was confirmed in an experiment run without any catalyst, where a conversion below 1% was determined after 36 h in CDCl₃. This implies that the auxiliary base Et₃N (**2**) present in the reaction mixture is not catalytically active.

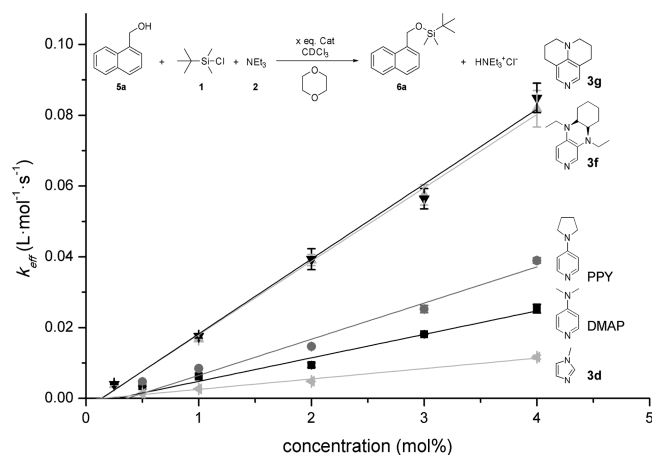
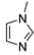
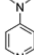
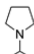
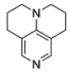
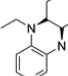


Figure 5. Correlations of effective rate constant k_{eff} vs catalyst concentration for the silylation of alcohol **5a** using DMAP, PPY, **3d**, **3f**, and **3g** as catalysts.

Table 3. Silyl Cation Affinities (SCAs) and Effective Rate Constants k'_{eff} for the Silylations of Primary Alcohol **5a** and Secondary Alcohol **5b** Using Different Catalysts

Catalyst	SCA ^[a] [CHCl ₃]	k'_{eff} 5a ^[b]	k'_{eff} 5b ^[b]	k'_{eff} 5a / k'_{eff} 5b
 3d	-32.4	$2.94 \cdot 10^{-3}$	$5.76 \cdot 10^{-5}$	51.0
 3a	-43.1	$6.63 \cdot 10^{-3}$	$5.39 \cdot 10^{-5}$	123.0
 3b	-47.4	$1.02 \cdot 10^{-2}$	$7.83 \cdot 10^{-5}$	130.3
 3g	-56.5	$2.12 \cdot 10^{-2}$	$1.68 \cdot 10^{-4}$	126.2
 3f	-62.0	$2.08 \cdot 10^{-2}$	$1.47 \cdot 10^{-4}$	141.5

^aSilyl cation affinities at 298.15 K (in kJ/mol) in CHCl₃. ^[b] k'_{eff} in L·mol⁻¹·s⁻¹.

Theoretical Evaluation of the Silyl Transfer Enthalpy.

In order to establish a possible link between the catalytic efficiency and the Lewis basicity of the catalyst, the affinity of each catalyst toward the *tert*-butyldimethylsilyl cation at 298.15 K was calculated at the MP2(FC)/G3MP2large//MPW1K/6-31+G(d) level of theory (Table 2). Solvent effects in CHCl₃ were computed at the PCM/UAHF/MPW1K/6-31+G(d) level of theory. The silyl cation affinities (SCAs) were determined relative to that for pyridine as the reference base using the isodesmic silyl group transfer reaction shown in Figure 6. The SCA of -24.7 kJ/mol for imidazole (**3c**) thus implies that the *tert*-butyldimethylsilyl group attaches to imidazole 24.7 kJ/mol more strongly than to pyridine. The calculations yielded the lowest SCA values for the least effective catalysts **3c** and **3d**, higher values for the more efficient catalysts DMAP and PPY,

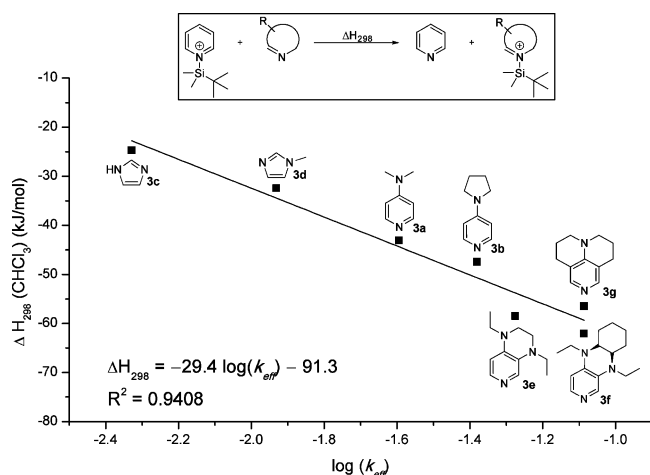


Figure 6. Plot of silyl cation affinity (relative to the reference base pyridine) vs $\log(k_{\text{eff}})$ for the silylation of alcohol **5a** with various catalysts in CHCl_3 .

and the highest values for the most active catalysts, pyridines **3e**, **3f**, and **3g**. Despite the fact that the correlation between SCA values and reaction rates is not perfect for the group of highly active catalysts, the trend of higher catalytic reactivity for the more Lewis basic catalysts is in line with expectation for the mechanism shown in Scheme 2 involving pre-equilibrium formation of the silylated catalyst and subsequent rate-limiting transfer of the silyl group to the substrate alcohol. A similar correlation has recently been observed for the Lewis base-catalyzed acylation of alcohols.¹⁵

Reaction with Secondary Alcohol 5b. Reaction rates for the secondary alcohol 1-(naphthalen-1-yl)ethanol (**5b**) were determined under conditions nearly identical to those for primary alcohol **5a**. As expected, the reaction rate for the silylation of **5b** is much lower than that for primary alcohol **5a**. With DMAP at a catalyst loading of 4 mol %, for example, the half-life for the silylation of primary alcohol **5a** is 30.2 min, while that for the silylation of secondary alcohol **5b** is 3166 min. This decrease of approximately 2 orders of magnitude in the absolute reaction rate was also observed for all of the other Lewis base catalysts investigated here (Table 3). Kinetic measurements were again repeated at various catalyst loadings, and linear correlations between k_{eff} and the catalyst concentration were also observed for secondary alcohol **5b** (Figure 7).

The effective rate constants k'_{eff} for the silylation of secondary alcohol **5b** extracted from the correlations in Figure 7 with the aid of eq 1 indicate that pyridines **3f** and **3g** are again the most effective catalysts, followed by PPY, **3d**, and DMAP. However, the difference between the most and least efficient catalysts (**3g** vs DMAP) amounts to a factor of only 3.1. This range is significantly smaller than that observed for the silylation of primary alcohol **5a**, which implies that the ratio of rate constants k'_{eff} for primary and secondary alcohols increases systematically with the calculated Lewis basicity of the catalyst (Table 3).

The original Corey procedure employs a reaction temperature of 35 °C in order to increase both the solubilities of the reaction components and the reaction rate. The silylation reaction of secondary alcohol **5b** was therefore repeated using catalyst **3f** at 30 mol % catalyst loading at different reaction temperatures in CDCl_3 (see the Supporting Information for

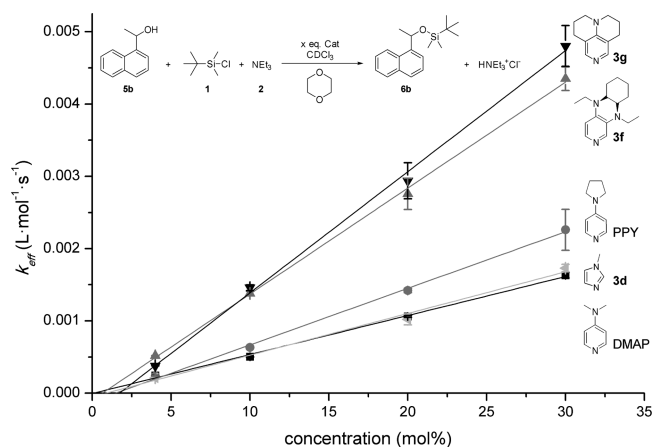


Figure 7. Correlations of rate constant k_{eff} vs catalyst concentration for the silylation of alcohol **5b** in CDCl_3 using DMAP, PPY, **3d**, **3f**, and **3g** as catalysts.

more information). As expected, the reaction rate increased for the benchmark reaction chosen here, providing reaction half-lives of 162.7 min at 23 °C and 129.1 min at 45 °C. Formal analysis of the moderately higher reaction rates at higher temperatures using an Eyring plot implies an activation enthalpy of $\Delta H^\ddagger = +5.8 \text{ kJ mol}^{-1}$ and an activation entropy of $\Delta S^\ddagger = -269.7 \text{ J K}^{-1} \text{ mol}^{-1}$. The value obtained for the activation enthalpy is quite small for a reaction in solution, whereas the negative value obtained for the activation entropy is typical for an effective third-order reaction. Similar results of $\Delta H^\ddagger = +12.8 \text{ kJ mol}^{-1}$ and $\Delta S^\ddagger = -240 \text{ J mol}^{-1} \text{ K}^{-1}$ have recently been determined for the PPY-catalyzed isobutyrylation of secondary alcohol **5b**.²⁷ Even though the Eyring plot is based on only three data points, the remarkable similarity of the activation parameters for the Lewis base-catalyzed silylation and acylation of alcohol **5b** points to an associative reaction mechanism in both cases.

Again with respect to the Corey procedure mentioned in the Introduction, we note that silylation reactions are often performed in polar aprotic solvents such as dimethylformamide (DMF) or dimethyl sulfoxide (DMSO). The influence of solvent polarity on the reaction rate was therefore studied for the silylation of secondary alcohol **5b** with TBSCl (**1**) in CD_2Cl_2 , CDCl_3 , and $\text{DMF-}d_7$ (Figure 8). With catalyst **3g** at 30 mol % loading and Et_3N (**2**) as the auxiliary base (1.2 equiv), the reaction was first studied in CDCl_3 and found to proceed with a half-life of 176.3 min. Repeating the reaction in CD_2Cl_2 under otherwise identical conditions yielded a slightly faster reaction with a half-life of 115.4 min. In contrast, the reaction in $\text{DMF-}d_7$ was found to be so much faster that accurate rate data could not be determined under these conditions. Omission of the catalyst as well as the auxiliary base eventually allowed accurate measurements but led to only 80% conversion. With Et_3N as the auxiliary base, full conversion was observed, and a half-life of 6.7 min was determined for $\text{DMF-}d_7$. Other solvents such as THF, acetone, and acetonitrile were also tested, but full analysis was impeded by formation of inhomogeneous reaction mixtures (most likely due to precipitation of $\text{Et}_3\text{NH}^+\text{Cl}^-$). The significant increase in the reaction rate in $\text{DMF-}d_7$ compared with the two halogenated solvents cannot be rationalized with common solvent parameters such as ET_{30} values or Gutman donor numbers

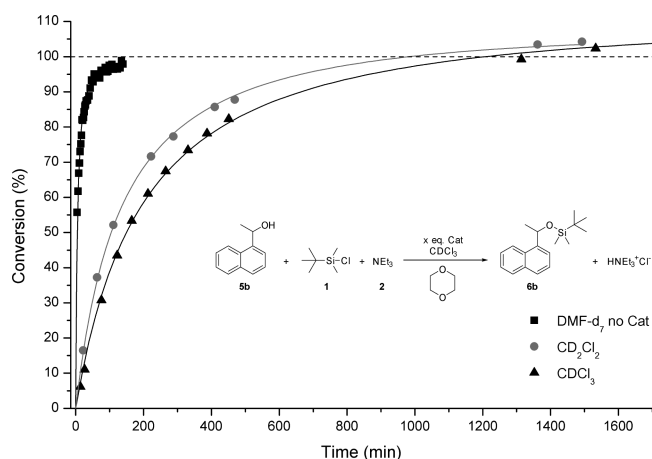


Figure 8. Reactions of secondary alcohol **5b** with TBSCl (**1**) in different solvents. The reactions in CDCl_3 and CD_2Cl_2 involved 30 mol % catalyst **3g** and Et_3N (1.2 equiv) as the auxiliary base, while the reaction in DMF-d_7 was performed without any catalyst.

and may better be understood in terms of the direct involvement of DMF-d_7 as a Lewis base catalyst.²⁸

In order to detect possible transient intermediates formed between silyl chloride **1** and Lewis base catalysts in reactions run in CDCl_3 or adducts with DMF-d_7 run in this latter solvent, the reaction progress was monitored using ^{29}Si NMR spectroscopy. Together with the results of numerous control experiments, the outcome of the ^{29}Si NMR measurements can be summarized as follows (Table 4 and Figure 9): (i) Transient

Table 4. ^{29}Si NMR Shifts (in ppm) of Several Compounds in CDCl_3 and DMF-d_7 in Comparison with Calculated ^{29}Si Shifts

entry	CDCl_3	DMF-d_7	^{29}Si calcd ^a
TBSCl (1)	36.10	37.11, 10.21	34.97
TBSCl (1) + Et_3N		37.11, 10.21	
TBSCl (1) + 5b		37.14, 18.32	
1 + AgSbF_6 (1 equiv)		41.88, 10.21	
1 + AgSbF_6 (0.5 equiv)		10.21	
6a	20.58	20.30	20.94
6b	18.43	18.48	20.22
6c	12.18	12.06	14.41
7	9.91	10.22	11.31
12	20.34	14.00	18.56
12b	20.39		17.19
12 + DMF (12c)		13.98, 10.25	13.95
TBSOTf (1b)	43.71, 9.9	41.97, 10.38	42.43
TBSOTf + 3a (i1)	33.25, 9.9		38.39
TBSOTf + 3g (i2)	32.16, 9.8		34.89
TBSOTf + DMF (i3)	44.06, 9.9		49.29

^aGeometries were obtained at the MPW1K/6-31+G(d) level of theory. ^{29}Si NMR shifts were calculated at the DF-LMP2/IGLO-III//MPW1K/6-31+G(d) level of theory.

ion pair intermediates formed between a Lewis base catalyst such as DMAP or pyridine **3g** and silyl chloride **1** could not be detected in CDCl_3 under the conditions of the benchmark reactions. Aside from silyl chloride **1** and silyl ether products **6a–c**, the only other detectable species under these conditions were small amounts of hydrolysis products [silanol **12**, which could be isolated and crystallized as hydrate **12b** (for details,

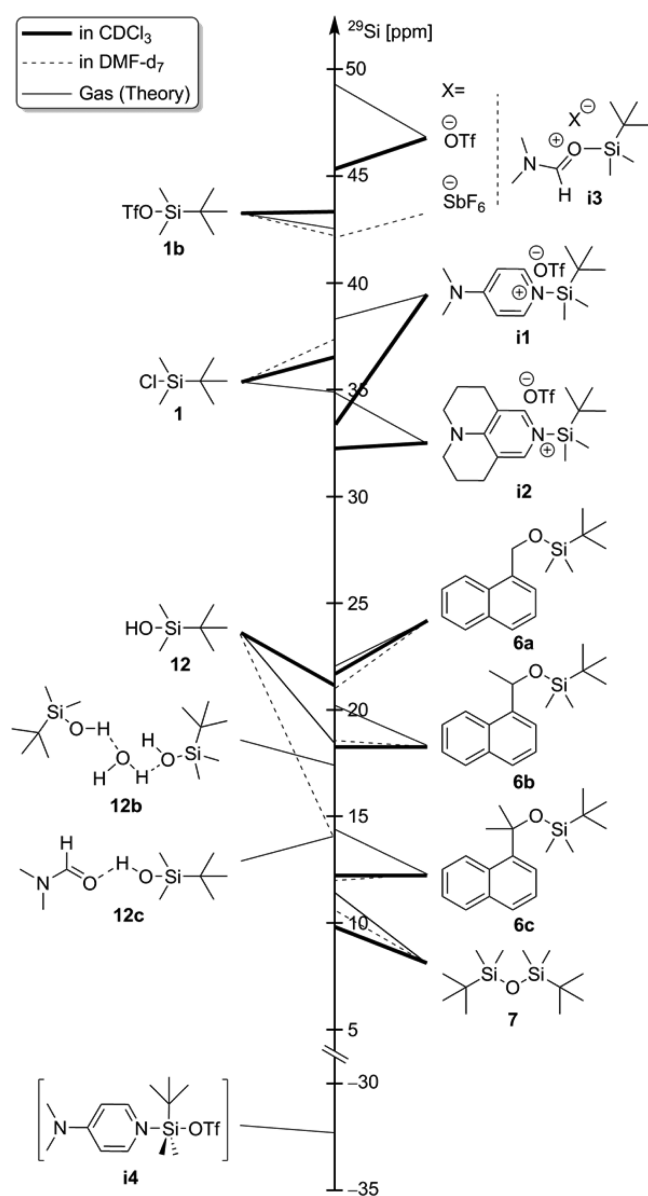


Figure 9. Comparison of ^{29}Si NMR results in CDCl_3 and DMF-d_7 with gas-phase calculations at the DF-LMP2/IGLO-III//MPW1K/6-31+G(d) level of theory.³²

see the Supporting Information), and bis(silyl) ether **7**]. Even mixtures of equimolar amounts of silyl chloride **1** and the Lewis base DMAP or pyridine **3g** did not lead to new signals in the ^{29}Si NMR spectrum. However, ion pair intermediates **i1** and **i2** were generated in CDCl_3 through the reaction of DMAP or **3g** with the more reactive silyl triflate **1b**. The new resonances observed at +33.25 ppm (for DMAP adduct **i1**) and +32.16 ppm (for **3g** adduct **i2**) can, together with results from ^1H , ^{13}C , and NOESY measurements, be assigned to the ion pair structures shown in Figure 9.^{29,30} These can also be located as true minima in gas-phase geometry optimizations at the MPW1K/6-31+G(d) level. However, the ^{29}Si chemical shifts predicted for **i1** and **i2** using a recently developed³² theoretical protocol are systematically shifted downfield by several parts per million.

(ii) Transient ion pair intermediates formed between DMF and silyl chloride **1** cannot be detected in DMF-d_7 under the conditions of the benchmark reaction shown in Figure 8. Aside from silyl chloride **1** and silyl ether product **6b**, the only other

detectable species were again the hydrolysis products **12** and **7**. Differences between ^{29}Si chemical shifts in CDCl_3 and $\text{DMF-}d_7$ are generally quite small unless specific solute–solvent interactions become important. This is the case for silanol **12**, whose ^{29}Si resonance moved from +20.4 ppm in CDCl_3 to +14.0 ppm in $\text{DMF-}d_7$ as a result of hydrogen-bonding interactions. This shift of 6 ppm was readily reproduced by ^{29}Si NMR shift calculations for silanol **12** and its DMF-bound complex **12c** (Figure 9).

However, the ^{29}Si NMR signal for silyl chloride **1** in $\text{DMF-}d_7$ at +37.1 ppm changed substantially upon addition of AgSbF_6 as a reagent for the precipitation of AgCl . The new resonance at +41.9 ppm obtained under these conditions was practically identical to that obtained for the more reactive silyl triflate **1b** in $\text{DMF-}d_7$, and can be attributed to ion pair **i3** (with either SbF_6 or triflate as the counterion; Figure 9).^{29–31} Ion pair **i3** (with triflate as the counterion) could again be located as a true minimum in gas-phase geometry optimizations at the MPW1K/6-31+G(d) level. As already observed for ion pairs **i1** and **i2**, the calculated ^{29}Si NMR signal predicted for **i3** is shifted downfield by several parts per million relative to that observed in $\text{DMF-}d_7$ solution. Attempts to identify ion pair intermediate **i3** also in CDCl_3 solution revealed an interesting temperature effect: while the ^{29}Si NMR signal for **i3** in $\text{DMF-}d_7$ solution remained effectively unchanged over the temperature range from -50 to $+70$ °C, a mixture of silyl triflate **1b** and DMF (1.5:1 ratio) in CDCl_3 showed signals for **i3** (+45.2 ppm) only at -50 °C. This signal vanished upon warming to room temperature, in line with expectations for the reversible formation of ion pair **i3**. Complementary observations can be made in the ^1H NMR spectrum, where the broad signals observed for DMF at room temperature at +8.55 and +3.46 ppm split into two sharp singlets at -50 °C.

(iii) Even though all of the ^{29}Si NMR evidence points to tetracoordinate silicon intermediates only, one should not dismiss the possibility of pentacoordinate silicon species or true silyl cation intermediates prematurely.³¹ A pentacoordinate isomer of ion pair **i1** (termed **i4**) could actually be identified as a local minimum on the MPW1K-D2/6-31+G(d) potential energy surface and was found to be located +42.8 kJ/mol higher compared with **i1**.³³ The calculated ^{29}Si chemical shift for **i4** amounts to -32.24 ppm, which is in line with predictions for other pentacoordinate silicon species.³⁴ Signals in this range of the ^{29}Si NMR spectrum were not detected in any of the measurements performed in this study, and we therefore exclude the formation of pentacoordinate intermediates in the reaction of DMAP with silyl triflate **1b**.

The auxiliary base plays an important role during the reaction in DMF. While the reaction reaches a plateau at 80% conversion in pure DMF, addition of 1.2 equiv of Et_3N (relative to alcohol **5b**) leads the reaction to full conversion. For the experiment in pure $\text{DMF-}d_7$, the ^{29}Si NMR spectrum shows signals of starting materials as well as product (Figure 10, top). After addition of Et_3N , only the product signal was observed in ^{29}Si NMR measurements.

These results imply that the reaction is inhibited by hydrogen chloride generated during the reaction process without auxiliary base and can resume when the acid is removed from the reaction mixture. The major role of imidazole in the Corey procedure described in the Introduction therefore seems to be more that of an auxiliary base (rather than that of a catalyst).

Reaction with Tertiary Alcohols. Finally, reaction rates were determined for silylation of alcohol **5c** with TBSCl (**1**)

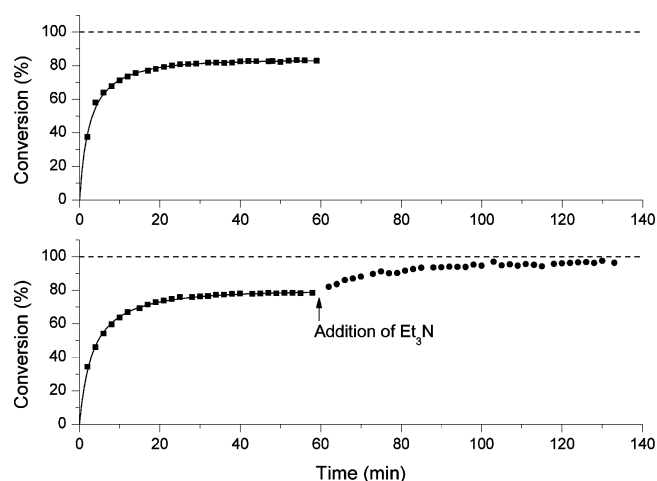


Figure 10. Kinetic measurements on **5b** in $\text{DMF-}d_7$ (top) with no catalyst and no auxiliary base and (bottom) with the addition of Et_3N (**2**) after 60 min of reaction.

using identical conditions as shown before in $\text{DMF-}d_7$ with 1.2 equiv of Et_3N as the auxiliary base and no catalyst. However, the reaction was very slow under these conditions: while full conversion was reached after several minutes for primary and secondary alcohols **5a** and **5b**, the first product signals for tertiary silyl ether **6c** were observed only after several hours of reaction time. On the basis of the data collected up to 55% conversion, one can predict a reaction half-life of $t_{1/2} = 109\,029$ min (or approximately 75 days) for tertiary alcohol **5c** (Figure 11). Repeating the reaction in the presence of catalyst **3g** (**30**)

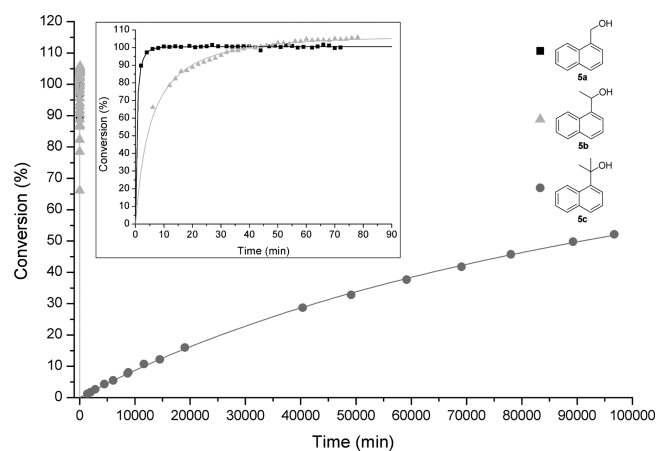


Figure 11. Conversion vs time plots for alcohols **5a**, **5b**, and **5c** in $\text{DMF-}d_7$ with Et_3N (1.2 equiv) as the auxiliary base and without any catalyst.

mol %) under otherwise identical conditions led to no acceleration of turnover, which again supports the Lewis basic solvent $\text{DMF-}d_7$ as the only catalytically active species under these conditions (see the Supporting Information for further information). This implies that the silyl chloride reagent **1** used here is intrinsically not reactive enough to turn over tertiary substrates in a synthetically meaningful way. However, the limited kinetic data available for alcohols **5a**, **5b**, and **5c** can be combined to extract relative reactivities of 404345:20232:1 for these three substrates under otherwise identical conditions ($\text{DMF-}d_7$, rt, Et_3N as the auxiliary base, no catalyst). This implies that the reactivity difference between secondary alcohol

5b and tertiary alcohol **5c** (a factor of 20 232) is much larger than the reactivity difference between primary alcohol **5a** and secondary alcohol **5b** (a factor of 20.0).

CONCLUSION

Among the various factors influencing the silylation of primary and secondary alcohols, the choice of solvent and catalyst are clearly the most important (and interdependent). In DMF as the solvent there is actually no need for added catalysts because of the high catalytic activity of this solvent alone. Despite the fact that direct detection of silylated DMF intermediates by ^{29}Si NMR spectroscopy has not been successful, the formation of these intermediates from silyl chlorides and DMF and their subsequent reaction with substrate alcohols remains the best mechanistic hypothesis. The reactions are much slower in apolar organic solvents such as dichloromethane (DCM) and chloroform, even in the presence of highly active catalysts. For the purpose of preparing silyl ethers of primary and secondary alcohols with the known silyl chloride reagents, the established Corey procedure thus still provides the most rapid and economical means. However, should the selective transformation of primary over secondary alcohols be the goal, the conclusions will be somewhat different, as already pointed out previously.⁵ The reactivity difference between primary and secondary alcohols amounts to 20.0 under DMF conditions, compared with 51 for *N*-methylimidazole (**3d**) in CDCl_3 and 120–145 for electron-rich pyridines such as **3g** and **3f** in CDCl_3 . When these ratios are plotted against the silyl cation affinities of the respective Lewis bases as in Figure 12, it

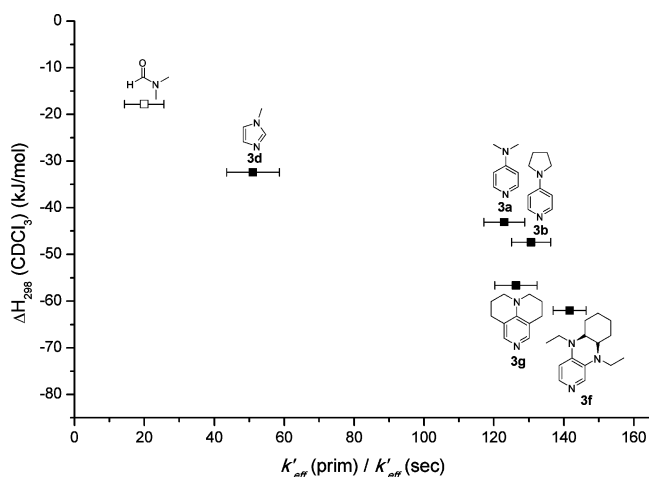


Figure 12. Calculated silyl cation affinities vs selectivity ratios of chosen catalysts. The ratio for DMF was determined from the measurements in DMF as the solvent.

becomes apparent that the stability of the Lewis base–silyl cation adducts are at least partially responsible for the observed selectivities: the least stable intermediate (silylated DMF) provides the lowest selectivities, while the much more stable silylpyridinium intermediates all yield selectivities greater than 100. The choice of auxiliary base or reaction temperature appears to be of minor importance in comparison.

The auxiliary base is needed in all of the protocols to neutralize the generated acid and guide the reaction to full conversion. In protocols employing pyridine catalysts, the auxiliary base is also needed to avoid catalyst deactivation through protonation. This role can be fulfilled by a variety of

amine bases such as Et_3N , TOA, and DIPEA. A moderate increase in the reaction temperature is helpful to solve solubility issues for certain substrates but otherwise leads to only moderate rate enhancements.

EXPERIMENTAL SECTION

General Methods. All air- and water-sensitive manipulations were carried out under a nitrogen atmosphere using standard Schlenk techniques. Calibrated flasks for kinetic measurements were dried in the oven at $120\text{ }^\circ\text{C}$ for at least 12 h prior to use and then assembled quickly while still hot, cooled under a nitrogen stream, and sealed with a rubber septum. Commercial chemicals were of reagent grade and were used as received, unless otherwise noted. CDCl_3 was refluxed for at least 1 h over CaH_2 and subsequently distilled. ^1H and ^{13}C NMR spectra were recorded at room temperature. All ^1H chemical shifts are reported in parts per million (δ) relative to CDCl_3 (δ 7.26); ^{13}C chemical shifts are reported in parts per million (δ) relative to CDCl_3 (δ 77.16). ^1H NMR kinetic data were measured on a 200 MHz spectrometer at $23\text{ }^\circ\text{C}$. HRMS spectra (ESI-MS or EI-MS) were obtained using an FT instrument. For all of the kinetic measurements with reaction times longer than 24 h, the reaction mixtures were mechanically shaken at room temperature. For each reaction, the rotation speed was set at 480 turns/min. Analytical TLC was carried out using aluminum sheets coated with silica gel 60 F254. All other chemicals were purchased from commercial suppliers at the highest available grade, stored over orange gel in a desiccator, and used without any further purification.

General Procedure I for Benchmark Reactions of 5a with 2 mol %/3 mol %/4 mol % Catalyst. A 0.2 mL aliquot from 5.0 mL of stock solution I [TBSCl (542 mg, 3.6 mmol), dioxane (0.088 g, 0.086 mL)], 0.2 mL from 5 mL of stock solution II [**5a** (475 mg, 3.0 mmol), Et_3N (364 mg, 0.50 mL)], and 0.2 mL from 5 mL of stock solution III (0.06/0.09/0.12 mmol of catalyst) were mixed in an NMR tube and sealed.

General Procedure II for Benchmark Reactions of 5a with 0.25 mol %/0.5 mol % Catalyst. A 0.2 mL aliquot from 5.0 mL of stock solution I [TBSCl (542 mg, 3.6 mmol), dioxane (0.088 g, 0.086 mL)], 0.2 mL from 5 mL of stock solution II [**5a** (475 mg, 3.0 mmol), Et_3N (364 mg, 0.50 mL)], and 0.2 mL from 10 mL of stock solution III (0.015/0.030/0.060 mmol of catalyst) were mixed in an NMR tube and flame-sealed.

General Procedure III for Benchmark Reactions of 5b with 4 mol %/10 mol %/20 mol %/30 mol % Catalyst. A 0.2 mL aliquot from 5.0 mL of stock solution I [TBSCl (1.54 mg, 3.6 mmol), dioxane (0.088 g, 0.086 mL)], 0.2 mL from 5 mL of stock solution II [**5b** (517 mg, 3.0 mmol), Et_3N (2.36 mg, 0.50 mL)], and 0.2 mL of 2 mL stock solution III (0.048/0.12/0.24/0.36 mmol of catalyst) were mixed in an NMR tube and flame-sealed.

General Procedure IV for Temperature-Dependent Reactions of 5b with 30 mol % Catalyst 3f. A 0.2 mL aliquot from 5.0 mL of stock solution I [TBSCl (1.54 mg, 3.6 mmol), dioxane (0.088 g, 0.086 mL)], 0.2 mL from 5 mL of stock solution II [**5b** (517 mg, 3.0 mmol), Et_3N (2.36 mg, 0.50 mL)], and 0.2 mL from 2 mL of stock solution III (0.36 mmol of catalyst **3f**) were mixed in an NMR tube and flame-sealed. During the NMR measurement the temperature was set to the temperature of choice.

Naphthalen-1-ylmethanol (5a). NaBH_4 (0.567 g, 15 mmol, 0.5 equiv) was dissolved in 100 mL of THF, and the solution was cooled to $-10\text{ }^\circ\text{C}$. 1-Naphthaldehyde (4.68 g, 30 mmol, 4.07 mL, 1.0 equiv) was dissolved in 50 mL of THF, and this solution was added dropwise to the reaction mixture. The reaction mixture was allowed to stir for 30 min at rt, and the reaction process was monitored by TLC. The reaction was quenched by addition of 2 M HCl until no H_2 appeared. The reaction mixture was extracted three times with DCM (20 mL) and washed with brine (20 mL). The combined organic phases were dried over MgSO_4 , and the solvent was removed under reduced pressure. Column chromatography on silica (hexane/EtOAc, 4:1) led to a white solid product **5a** in 95% yield (4.50 g). ^1H NMR (300 MHz, CDCl_3): δ 2.67 (bs, 1H, OH), 5.05 (s, 2H, CH_2), 7.40–7.61 (m, 4H),

7.81–7.87 (m, 1H), 7.88–7.96 (m, 1H), 8.03–8.14 (m, 1H). ¹³C NMR (75 MHz, CDCl₃): δ 63.4, 123.7, 125.3, 125.9, 126.3, 128.5, 128.7, 131.3, 133.8, 136.3. MS (EI) *m/z* (%): 158.1 ([M + H]⁺, 83), 141.1 ([M – OH]⁺, 20), 129.2 ([M – CH₂OH]⁺, 100). HRMS (EI): C₁₁H₁₀O requires 158.0732 g/mol, found 158.0726 g/mol.

2-(Naphthalen-1-yl)propan-2-ol (5c). Magnesium (2.38 g, 100 mmol) and LiCl (2.08 g, 50 mmol) were dissolved in 150 mL of THF, and a little bit of iodine was added. The reaction mixture was allowed to stir for 15 min. 1-Bromonaphthalene (8.22 g, 40 mmol) was added slowly, and the mixture was stirred for 30 min and refluxed for 1 h. The reaction mixture was cooled to rt, and acetone (4.64 g, 80 mmol) was added slowly. After 1 h of stirring at rt, the mixture was refluxed for 3 h. The reaction was quenched by addition of saturated NH₄Cl under ice cooling. The reaction mixture was extracted three times with DCM (50 mL) and washed with brine (20 mL). The combined organic phases were dried over MgSO₄, and the solvent was removed under reduced pressure. Recrystallization from *n*-hexane led to a white solid product **5c** in 82% yield (6.1 g). ¹H NMR (300 MHz, CDCl₃): δ 1.89 (s, 6H), 7.36–7.74 (m, 4H), 7.80 (d, *J* = 8.1 Hz, 1H), 7.85–7.98 (m, 1H), 8.76–9.01 (m, 1H). ¹³C NMR (75 MHz, CDCl₃): δ 31.6, 74.1, 122.7, 124.8, 125.2, 125.3, 127.4, 128.6, 129.1, 131.0, 134.9, 143.4. MS (GC/EI) *m/z* (%): 186.23 ([M + H]⁺, 54), 171.20 ([M – CH₃]⁺, 100), 153.19 ([M – CH₃ – CH₃]⁺, 32), 128.16 ([M – (CH₃)₂COH]⁺, 22). HRMS (GC/EI): C₁₃H₁₄O requires 186.1045 g/mol, found 186.1036 g/mol.

tert-Butyldimethyl(naphthalen-1-ylmethoxy)silane (6a). Naphthalen-1-ylmethanol (0.32 g, 2 mmol) and **1** (0.36 g, 2.4 mmol) were dissolved in 15 mL of DCM, and Et₃N (0.33 mL, 0.24 g, 2.4 mmol) was added. After addition of DMAP (0.01 g, 0.08 mmol), the reaction mixture was stirred at rt for 12 h. The mixture was washed with sat. aq. NH₄Cl solution and extracted with DCM (3 × 5 mL), and the combined organic phases were dried over MgSO₄. The solvent was removed under reduced pressure. Column chromatography (*n*-hexane/DCM, 4:1) yielded 0.44 g of **6a** (1.62 mmol, 82%) as a colorless oil. ¹H NMR (300 MHz, CDCl₃): δ 0.14 (s, 6H, Si(CH₂)₂), 0.97 (s, 9H, SiBu), 5.22 (s, 2H, CH₂), 7.47–7.59 (m, 3H), 7.59–7.61 (m, 1H), 7.79 (d, *J* = 8.1 Hz, 1H), 7.86–7.93 (m, 1H), 8.00–8.05 (m, 1H). ¹³C NMR (75 MHz, CDCl₃): δ –5.2, 18.5, 26.0, 29.2, 63.4, 123.3, 123.8, 125.45, 125.51, 125.8, 127.5, 128.6. ²⁹Si NMR (80 MHz, CDCl₃): δ 20.58. MS (EI) *m/z* (%): 272.17 ([M], 0.6), 215.09 ([M – tBu]⁺, 72), 141.07 ([M – OTBS]⁺, 100) 115.05 ([TBS]⁺, 13). HRMS (EI): C₁₇H₂₄OSi requires 272.1596, found 272.1590.

tert-Butyldimethyl(1-(naphthalen-1-yl)ethoxy)silane (6b). 1-(Naphthalen-1-yl)ethanol (0.35 g, 2 mmol) and **1** (0.36 g, 2.4 mmol) were dissolved in 15 mL of DCM, and triethylamine (0.33 mL, 0.24 g, 2.4 mmol) was added. After addition of DMAP (0.01 g, 0.08 mmol), the reaction mixture was stirred at rt for 48 h. The mixture was washed with sat. aq. NH₄Cl solution and extracted with DCM (3 × 5 mL), and the combined organic phases were dried over MgSO₄. The solvent was removed under reduced pressure. Column chromatography (*n*-hexane/DCM, 4:1) yielded 0.46 g of **6b** (1.52 mmol, 76%) as a colorless oil. ¹H NMR (300 MHz, CDCl₃): δ –0.01 (s, 3H, SiCH₃tBu), 0.10 (s, 3H, SiCH₃tBu), 0.95 (s, 9H, SiBu), 1.60 (d, *J* = 6.4 Hz, 3H, CH₃CHOR), 5.61 (q, *J* = 6.6 Hz, 1H, CH), 7.44–7.55 (m, 3H), 7.67–7.78 (m, 2H), 7.85–7.91 (m, 1H), 8.11 (d, *J* = 7.3 Hz, 1H). ¹³C NMR (75 MHz, CDCl₃): δ –4.8, –4.9, 18.3, 25.9, 26.6, 68.5, 122.7, 123.3, 125.2, 125.5, 125.6, 127.2, 128.8, 129.9. ²⁹Si NMR (80 MHz, CDCl₃): δ 18.43. MS (EI) *m/z* (%): 215.16 (6), 155.17 ([M – C₆H₁₅OSi], 23), 141.15 (33), 115.14 ([C₆H₁₅Si], 13), 76.09 ([C₆H₄], 27), 75.09 ([C₆H₃], 100). HRMS (EI): C₁₈H₂₆OSi requires 286.1753, found 286.1744.

tert-Butyldimethyl(2-(naphthalen-1-yl)propan-2-yl)oxy)silane (6c). 2-(Naphthalen-1-yl)propan-2-ol (0.37 g, 2 mmol) and imidazole (1.36 g, 20 mmol) were dissolved in 10 mL of DMF, and **1** (1.51 g, 10 mmol) was slowly added. The reaction mixture was stirred at rt for 12 h and at 70 °C for 7 days. The mixture was washed with sat. aq. NH₄Cl solution, extracted with DCM (3 × 10 mL), and washed once with brine, and the combined organic phases were dried over MgSO₄. The solvent was removed under reduced pressure. Column chromatography (*n*-hexane) yielded 0.3 g of **6c** (1.00 mmol, 50%) as a colorless oil. ¹H NMR (300 MHz, CDCl₃): δ –0.14 (s, 6H,

Si(CH₂)₂), 0.91 (s, 9H, SiBu), 1.89 (s, 6H, (CH₃)₂), 7.36–7.53 (m, 3H), 7.55 (dd, *J* = 7.3, 1.2 Hz, 1H), 7.74–7.77 (m, 1H), 7.84–7.87 (m, 1H), 8.82–8.85 (m, 1H). ¹³C NMR (75 MHz, CDCl₃): δ –2.2, 18.6, 26.3, 32.7, 76.4, 122.5, 124.8, 124.9, 125.1, 128.4, 128.8, 128.9, 131.3, 134.9, 144.2. ²⁹Si NMR (80 MHz, CDCl₃): δ 12.18. MS (EI) *m/z* (%): 285.17 ([M – CH₃], 2), 185.08 ([M – TBS], 10), 169.09 ([M – OTBS], 13), 127.06 ([M – Naph], 3), 75.09 ([C₆H₃], 100), 57.07 ([M – tBu], 5). HRMS (EI): C₁₈H₂₅OSi (**6c** –CH₃) requires 285.1675, found 285.1662.

1,3-Di-tert-butyl-1,1,3,3-tetramethyldisiloxane (7). **1** (2.00 g, 13.4 mmol) was dissolved in 5 mL of acetonitrile and 1 mL of H₂O. After the addition of KI (2.49 g, 15.0 mmol), the mixture was stirred at rt for 12 h. The upper layer was pipetted off and distilled (80 °C, 15 mbar; oil bath: 100 °C) affording 0.95 g of **7** (3.85 mmol, 28.7%) as a colorless liquid. ¹H NMR (300 MHz, CDCl₃): δ 0.85 (s, 18H, SiCH₃tBu), 0.00 (s, 12H, (CH₃)₂SiBu). ¹³C NMR (75 MHz, CDCl₃): δ 25.7, 18.1, –3.0. ²⁹Si NMR (80 MHz, CDCl₃): δ 9.91. MS (EI) *m/z* (%): 246.02 ([M]⁺, 0.02), 189.11 ([M – tBu], 2.8), 147.05 (100), 73.04 ([M – tBu(CH₃)₂Si], 1.9). HRMS (EI): C₁₂H₃₀Si₂O requires 246.1835, found 246.1828.

Di-tert-butyldimethylsilanol Hydrate (12b). Potassium hydroxide (0.18 g, 2.4 mmol) was dissolved in 1 mL of H₂O and 0.25 mL of methanol, and the solution was stirred at 0 °C. **1** (0.38 g, 2.5 mmol) was dissolved in 2 mL of diethyl ether, and this solution was slowly added to the reaction mixture. The reaction mixture was stirred for 10 min. The product was extracted three times with diethyl ether, and the solvent was removed under reduced pressure. Slow removal of the solvent led to the desired crystallized product. ¹H NMR (300 MHz, CDCl₃): δ 1.52 (s, 2H, H₂O), 0.89 (s, 18H, SiCH₃tBu), 0.07 (s, 12H, (CH₃)₂SiBu). ¹³C NMR (75 MHz, CDCl₃): δ 25.8, 17.9, –3.6. ²⁹Si NMR (80 MHz, CDCl₃): δ 20.39.

■ ASSOCIATED CONTENT

📄 Supporting Information

Explanation of methods, theoretical calculations, time conversion plots, NMR spectra, and the CIF file for compound **12b**. This material is available free of charge via the Internet at <http://pubs.acs.org>.

■ AUTHOR INFORMATION

Corresponding Author

*E-mail: zipse@cup.uni-muenchen.de

Notes

The authors declare no competing financial interest.

■ REFERENCES

- (1) (a) Wuts, P. G. M.; Greene, T. W. *Greene's Protective Groups in Organic Synthesis*, 4th ed.; John Wiley & Sons: Hoboken, NJ, 2006. (b) Kocienski, P. J. *Protecting Groups*, 3rd ed.; Thieme: Stuttgart, Germany, 2005.
- (2) White, J. D.; Carter, R. G. Silyl Ethers. In *Science of Synthesis*; Fleming, I., Ed.; Thieme: Stuttgart, Germany, 2002.
- (3) Crouch, D. *Synth. Commun.* **2013**, *43*, 2265–2279.
- (4) Venkateswarlu, A.; Corey, E. J. *J. Am. Chem. Soc.* **1972**, *94*, 6190–6191.
- (5) Chaudhary, S. K.; Hernandez, O. *Tetrahedron Lett.* **1979**, *20*, 99–102.
- (6) Kim, S.; Chang, H. *Synth. Commun.* **1984**, *14*, 899–904. Kim, S.; Chang, H. *Bull. Chem. Soc. Jpn.* **1985**, *58*, 3669–3670.
- (7) Lissel, M.; Weiffen, J. *Synth. Commun.* **1981**, *11*, 545–549.
- (8) Lombardo, L. *Tetrahedron Lett.* **1984**, *25*, 227–228.
- (9) Braish, T. F.; Fuchs, P. L. *Synth. Commun.* **1986**, *16*, 111–115.
- (10) (a) Akiba, K.-y.; Iseki, Y.; Wada, M. *Bull. Chem. Soc. Jpn.* **1984**, *57*, 1994–1999. (b) Akiba, K.-y.; Iseki, Y.; Wada, M. *Tetrahedron Lett.* **1982**, *23*, 3935–3936.
- (11) (a) Held, I.; Larionov, E.; Bozler, C.; Wagner, F.; Zipse, H. *Synthesis* **2009**, 2267–2277. (b) Held, I.; Villinger, A.; Zipse, H.

Synthesis **2005**, 1425–1430. (c) Wei, Y.; Held, I.; Zipse, H. *Org. Biomol. Chem.* **2006**, *4*, 4223–4230.

(12) (a) Müller, C. E.; Schreiner, P. R. *Angew. Chem., Int. Ed.* **2011**, *50*, 6012–6042. (b) Vedejs, E.; Jure, M. *Angew. Chem., Int. Ed.* **2005**, *44*, 3974–4001. (c) Wurz, R. P. *Chem. Rev.* **2007**, *107*, 5570–5595. (d) Spivey, A. C.; Arseniyadis, S. *Top. Curr. Chem.* **2009**, *291*, 233–280.

(13) Xu, S.; Held, I.; Kempf, B.; Mayr, H.; Steglich, W.; Zipse, H. *Chem.—Eur. J.* **2005**, *11*, 4751–4757.

(14) Heinrich, M. R.; Klisa, H. S.; Mayr, H.; Steglich, W.; Zipse, H. *Angew. Chem., Int. Ed.* **2003**, *42*, 4826–4828.

(15) Larionov, E.; Achraimer, F.; Humin, J.; Zipse, H. *ChemCatChem* **2012**, *4*, 559–566.

(16) De Rycke, N.; Couty, F.; David, O. R. P. *Chem.—Eur. J.* **2011**, *17*, 12852–12871.

(17) Baidya, M.; Kobayashi, S.; Brotzel, F.; Schmidhammer, U.; Riedle, E.; Mayr, H. *Angew. Chem., Int. Ed.* **2007**, *46*, 6176–6179.

(18) Soovaali, L.; Rodima, T.; Kaljurand, I.; Kuett, A.; Koppel, I.; Leito, I. *Org. Biomol. Chem.* **2006**, *4*, 2100–2105.

(19) Ibrahim, I. T.; Williams, A. J. *Chem. Soc., Perkin Trans. 2* **1982**, 1459–1466.

(20) Mayer, B. J.; Spencer, T. A.; Onan, K. D. *J. Am. Chem. Soc.* **1984**, *106*, 6343–6348.

(21) Pawelka, Z.; Zeegers-Huyskens, T. *Can. J. Chem.* **2003**, *81*, 1012–1018.

(22) Fujii, T.; Nishida, H.; Abiru, Y.; Yamamoto, M.; Kise, M. *Chem. Pharm. Bull.* **1995**, *43*, 1872–1877.

(23) Virtanen, N.; Polari, L.; Väililä, M.; Mikkola, S. *J. Phys. Org. Chem.* **2005**, *18*, 385–397.

(24) Hibbert, F.; Hunte, K. P. *J. Chem. Soc., Perkin Trans. 2* **1983**, 1895–1899.

(25) (a) Singh, S.; Das, G.; Singh, O. V.; Han, H. *Tetrahedron Lett.* **2007**, *48*, 1983–1986. (b) Held, I.; Xu, S.; Zipse, H. *Synthesis* **2007**, 1185–1196.

(26) (a) Fischer, C. B.; Xu, S.; Zipse, H. *Chem.—Eur. J.* **2006**, *12*, 5779–5784. (b) Tandon, R.; Unzner, T.; Nigst, T. A.; De Rycke, N.; Mayer, P.; Wendt, B.; David, O. R. P.; Zipse, H. *Chem.—Eur. J.* **2013**, *19*, 6435–6442. (c) Lindner, C.; Tandon, R.; Liu, Y.; Maryasin, B.; Zipse, H. *Org. Biomol. Chem.* **2012**, *10*, 3210–3218.

(27) (a) Larionov, E.; Mahesh, M.; Spivey, A. C.; Wei, Y.; Zipse, H. *J. Am. Chem. Soc.* **2012**, *134*, 9390–9399. (b) Vedejs, E.; Daugulis, O.; Harper, L. A.; MacKay, J. A.; Powell, D. R. *J. Org. Chem.* **2003**, *68*, 5020–5027.

(28) (a) Reichardt, C. *Chem. Rev.* **1994**, *94*, 2319–2358. (b) Gutmann, V. *Coord. Chem. Rev.* **1976**, *18*, 225–255.

(29) Bassindale, A. R.; Stout, T. *Tetrahedron Lett.* **1985**, *26*, 3403–3406.

(30) (a) Bassindale, A. R.; Stout, T. *J. Chem. Soc., Perkin Trans. 2* **1986**, 221–225. (b) Bassindale, A. R.; Lau, J. C.-Y.; Stout, T.; Taylor, P. G. *J. Chem. Soc., Perkin Trans. 2* **1986**, 227–231.

(31) (a) Lambert, J.; Zhao, Y.; Zhang, S. M. *J. Phys. Org. Chem.* **2001**, *14*, 370–379. (b) Chult, C.; Corriu, R. J. P.; Reye, C.; Young, J. C. *Chem. Rev.* **1993**, *93*, 1371–1448. (c) Dilman, A. D.; Ioffe, L. *Chem. Rev.* **2003**, *103*, 733–772.

(32) The methodological analysis of different theoretical approaches is described in: Zhang, C.; Patschinski, P.; Panisch, R.; Wender, J. H.; Holthausen, M.; Zipse, H. *Phys. Chem. Chem. Phys.* **2014**, *16*, 16642–16650.

(33) The pentacoordinate intermediate **i4** exists as a local minimum only on the MPW1K/6-31+G(d)+D2 and MP2(FC)/6-31+G(d) potential energy surfaces. Reoptimization of this structure at the MPW1K/6-31+G(d) level (i.e., without the added D2 dispersion correction) leads back to ion pair intermediate **i1**.

(34) (a) Arshadi, M.; Johnels, D.; Edlund, U.; Ottosson, C.-H.; Cremer, D. *J. Am. Chem. Soc.* **1996**, *118*, 5120–5131. (b) Reed, C. A. *Acc. Chem. Res.* **1998**, *31*, 325–332. (c) Kinrade, S. D.; Deguns, E. W.; Gillson, A.-M. E.; Knight, C. T. G. *Dalton Trans.* **2003**, 3713–3716. (d) Holmes, R. R. *Chem. Rev.* **1996**, *96*, 927–950.